Dynamics of the ordered structure formation in a thermal dusty plasma

Yaroslav K. Khodataev, Sergei A. Khrapak, Anatoli P. Nefedov, and Oleg F. Petrov
High Energy Density Research Center, Russian Academy of Sciences, Izhorskaya 13/19, 127412 Moscow, Russia
(Received 7 October 1997)

The dynamics of the ensemble of interacting dust grains under conditions of thermal plasma was studied, and the formation of the liquidlike structure observed in the experiment was investigated. The simulation results showed that ordering of the dust structure manifested in the experiment with thermal dusty plasmas can be explained by the electric interaction of dust grains. It is found that the structure obtained in the experiment is far from equilibrium because the plasma flight time is less than the time of structure formation. It conforms to the emergence of the experimental correlation function characterized by a sharp main peak with no high-order ones. It is shown through experimental measurements of the diffusion coefficient that the thermal energy of dust grains is close to the gas temperature, and the friction force acting on grains is determined via the expression obtained in the kinetic limit. [S1063-651X(98)03606-X]

PACS number(s): 52.25.−b, 52.30.−q, 64.70.−p

I. INTRODUCTION

The physics of dusty plasma has seen much progress in recent years. One of the reasons for the interest in this area is the formation of ordered structures of dust particles found recently in the laboratory. This process is attributed to the strong electrostatic interaction between charged dust particles. So-called dust crystals and dust liquids were obtained in the laboratory by different research groups [1–5] showing these structures to be one of the typical phenomena in dusty plasma. It is now recognized that this material, the structure of which can actually be seen by laser scattering, may contribute not only to the plasma physics, but also could be a valuable tool for studying physical processes in condensed matter, such as melting, annealing, and lattice defects.

Most of the experiments on dust ordering were carried out in a plasma of radio-frequency (rf) gas discharge [1–4]. The formation of macroscopic ordered structures was found also in the standing strata of a direct current glow discharge [5]. Under conditions of discharge experiments dust grains acquire negative charge because the flux of electrons to an uncharged particle surface is high relative to that of ions.

Shown recently was the formation of dust ordered structures in thermal dusty plasma under atmospheric pressure and temperatures of 1700–2200 K [6]. The thermal plasma was weakly ionized with electrons, ions, and gas all having the same temperature. When dust particles are introduced into thermal plasma they become charged by collecting electrons and ions, as they do in discharges, but also by emitting electrons. The latter process can lead to a positive electric charge, unlike the negative charges in low-pressure discharge experiments. The experimental facility incorporated the plasma device and the diagnostic instrumentation for determination of plasma and gas parameters (see [6] for more details about experimental setup and procedure). The dusty plasma device produces the laminar spray of thermal dusty plasma under atmospheric pressure. It was possible to make a number of measurements of dusty plasma parameters such as the electron n_e and ion n_i number densities, plasma temperature T_g, and the diameter a and number density n_d of particles. The time-of-flight laser system was employed to analyze the particle structure in the thermal spray and then to compute the radial pair correlation function. The photon correlation spectroscopy method was used to systematically study the dynamics of charged dust grains in the plasma.

In Ref. [6] it was shown that the pair correlation function of CeO_2 particles computed at the plasma temperature $T_g = 1700$ K and particle number density $n_d = 5 \times 10^7$ cm^{-3} reveals the distinctive short-range order of a liquid system. The particle charge Q_d determined by charge balance is positive and its value is about 500 elementary charges [6]. The estimated corresponding coupling parameter, which is the ratio of the Coulomb electrostatic interaction energy to the dust thermal energy is $\Gamma \approx 150$. Such a Γ value is high enough to expect the ordered structure formation as the dust system appears to be essentially strongly coupled in this case.

The conditions and procedure of the experiment described differ essentially from that of the discharge experiments giving hope to enrich our knowledge of the dust structuring processes. In particular, one of the attractive features of the thermal dusty plasma is the relative simplicity of the uniform conditions. It is an obvious advantage as compared to the rf-discharge situation where the plasma crystal forms near the bottom electrode at the boundary of the cathode sheath, which is a strongly nonuniform and anisotropic region. This circumstance means that the theoretical interpretation of the structure obtained can turn out to be easier in the case of the thermal dusty plasma than in the case of the discharge one. Another advantage is the developed diagnostic base supporting the experiment.

The main idea of this paper is to study the dynamics of the ensemble of interacting dust grains, in particular, to investigate the formation of the liquidlike structure observed in the experiment. The correct numerical simulation requires verification of the dusty plasma parameters that are not measured directly, in particular, the dust thermal energy, friction coefficient of dust grains, and characteristic time of dust charging. The values of the dust thermal energy and friction coefficient are obtained by means of photon correlation spectroscopy (Sec. II). The characteristic dust charging time is estimated by showing it to be small compared with the simulation time step (Sec. III).

The solution of the problem has also required some specific approach. The point is that in our case the particle system may not achieve the stationary state. The pair correlation function of the dust structure was measured at a height of approximately 35 mm over the burner surface. Taking into account the spray velocity (about 5 m/s) the estimate for the dusty plasma flight time is $t_{\mathrm{ft}} \approx 7$ ms. Therefore it is not obvious that the equilibrium pair correlation function can describe the dust structure observed in the experiment. The time evolution of the pair correlation function needs to be investigated. In order to do it the dynamics of the 2D system of interacting dust grains has been simulated by means of usual molecular dynamics (MD) method. However, the pair correlation function was calculated from the positions of the grains at the moment taken without any time averaging.

The simulation procedure is described in Sec. IV. The pair correlation function obtained in the simulation is compared with the experimental one. The absence of high-order peaks of the experimental pair correlation function and the broadening of its first peak are discussed.

II. DUST THERMAL ENERGY

In recent years, the problem of the dynamic properties of dust particles in plasmas has received detailed attention. In low temperature weak-ionized plasma the dust grain has a large surface area and effectively exchanges its kinetic energy with neutral atoms or molecules. Thus it is usually assumed that dust particles can be characterized by a neutral gas temperature and exhibit Brownian motion. However, recent investigations of the strongly coupled dusty plasma show that this assumption requires special verification. It was shown that at some conditions the temperature that characterizes random motion of dust grains can greatly exceed the neutral gas temperature [7–10]. The processes leading to the observed high particle temperatures are not known. So it is not obvious what the temperature characterizing the kinetic energy of dust particles is under our conditions.

To resolve this problem and to study the dynamics of CeO_2 particles in a laminar spray of thermal plasma the photon correlation spectroscopy (PCS) method was used. The basic idea of this technique is a measurement of characteristic fluctuation time through temporal correlation of the detected scattered light signal. The temporal autocorrelation function (AF) $G^{(2)}(\mathbf{k},\tau)$ is studied:

$$G^{(2)}(\mathbf{k},\tau)=\langle I(\mathbf{k},0)I(\mathbf{k},\tau)\rangle, \tag{1}$$

where I is the intensity of the scattered light, τ is the time, and $\mathbf{k}$ is the scattering wave vector the magnitude of which is

$$|\mathbf{k}|=\frac{4\pi n}{\lambda}\sin\left(\frac{\theta}{2}\right), \tag{2}$$

where n is the refractive index of the medium, λ is the wavelength of the incident light, and θ is the scattering angle.

If (a) the scattering volume contains a large number of particles so that this number does not fluctuate greatly, (b) multiple scattering can be neglected, (c) the particles are small and/or spherical, and possess no mean motion, and (d) their dynamics is governed by the diffusion equation, we can rewrite Eq. (1) in the following form [11,12]:

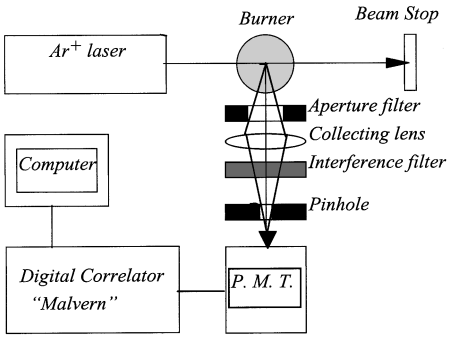

FIG. 1. Schematic representation of photon correlation system used in experiment (top view).

$$g^{(2)}(\tau)=1+\beta\,\exp(-2k^2D_d\tau), \tag{3}$$

where $g^{(2)}(\tau)$ is the normalized AF, and D_d is the diffusion coefficient of dust particles. The coherence factor β is smaller than 1 at finite apertures and reflects the degree of spatial coherence of the detected light.

When mean particle motion is significant (as in our experiment where the particles are moving in a laminar spray of thermal plasma) two additional requirements arise. It is desirable to make the Doppler term due to the flow velocity of the particles as unimportant as possible. This is done by adjusting the scattering plane perpendicular to the flow velocity [13]. Also, the analysis of two characteristic times τ_d (diffusion time) and τ_u (transit time through laser beam) is needed [14]:

$$\tau_d=\frac{1}{2k^2D_d}, \tag{4}$$

$$\tau_u=\frac{b}{u}, \tag{5}$$

where b is the characteristic length of scattering volume, and u is the flow velocity. In conditions where the particle mean motion dominates ($\tau_d \gg \tau_u$) the AF of scattered light intensity will provide information on flow velocity. If $\tau_d \ll \tau_u$ the particles may be assumed to possess no mean velocity and Eq. (3) is valid. As a general rule Eq. (3) may be used under conditions where [14]

$$\tau_d < 0.25\tau_u\,. \tag{6}$$

A schematic representation of the photon correlation system used in our experiment is shown in Fig. 1. The light source was the Ar^+ laser and the wavelength used was $\lambda=488$ nm. Scattering light is collected at 90° from the incident beam. Spatial filters were used to define the scattering volume. A collecting lens of 200 mm focal length was used to focus the image of the scattering volume on the surface of an EMI 9863KB/100 photomultiplier tube operating in the single-photon-counting mode. The counting pulses were processed with the Malvern Digital Correlator connected with the IBM PC/XT. The MALVERN software controls the correlator and extracts data from the measured AF.

We have obtained the autocorrelation functions of scattering light intensity for CeO_2 particles in an air flow at room temperature (without flame) and for a laminar spray of ther-

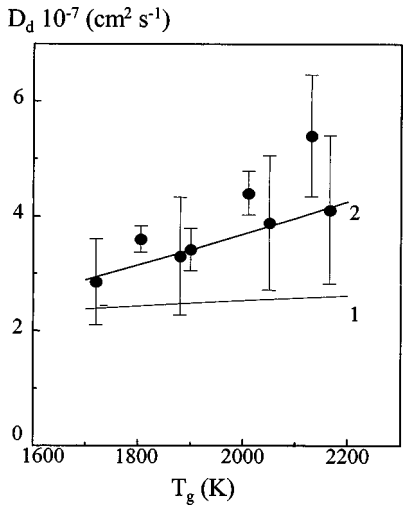

FIG. 2. Temperature dependence of particle diffusion coefficient D_d. Two curves are theoretical predictions [1, Eq. (7); 2, Eq. (8)].

mal plasma. Plasma temperature was varied from 1700 to 2200 K. We used the initial part of the AF curve to satisfy Eq. (6). It was found that the initial decay of the AF is well represented by Eq. (3), so we used Eq. (3) to obtain the diffusion coefficient of dust particles from the AF.

We have obtained $D_d = 1.3 \times 10^{-7}$ cm^2/s for the CeO_2 particles in an air flow. We can determine particle diameter a using the standard equation

$$D_d = \frac{T_g}{3\pi\eta a}, \tag{7}$$

where T_g is the neutral gas temperature and η is the viscosity of the medium. For typical parameters $T_g = 295$ K and $\eta = 18.4 \times 10^{-6}$ Pa s we found $a = 1.84$ μm. This result is in good agreement with the result obtained by the light extinction technique [6].

The dependence of D_d on plasma temperature is shown in Fig. 2. The plasma parameters were $n_d = 3.8 \times 10^5 - 2.3 \times 10^6$, $n_i = 3.2 \times 10^9 - 3 \times 10^{10}$, and $n_e = 4.6 \times 10^9 - 3.3 \times 10^{10}$ cm^{-3}. It can be noted that the change in plasma parameters does not affect strongly the value of the diffusion coefficient. To compare our experimental results with theory two curves are also shown in Fig. 2. The first one is the $D_d(T_g)$ obtained using Eq. (7) that is valid in the hydrodynamic limit when the mean free path λ_{fp} of the gas molecules is much less than the particle size ($\lambda_{fp} \ll a$). The second curve $D_d(T_g)$ is valid in the opposite kinetic case ($\lambda_{fp} \gg a$):

$$D_d = \frac{3T_g^{3/2}}{2Pa^2(2\pi M)^{1/2}}, \tag{8}$$

where P is the gas pressure and M is the mass of the gas molecules. In our experiments $\lambda_{fp} \approx 0.8$–1.1 μm, so that $\lambda_{fp} \sim a$ and it is not clear what the proper form of the diffusion coefficient is in the region intermediate between these two limits, hydrodynamic and kinetic. However, the second curve is more consistent with the experimental results.

Thus, it was shown that in our experiment that particle motion is governed by the diffusion equation, and that the value of the diffusion coefficient is close to the Brownian particle diffusion coefficient, calculated for the kinetic ($\lambda_{fp} \gg a$) region. It should be noted that the size of dust particles used and plasma parameters obtained in the experiment described in this section differ slightly from those of the experiment on dust ordering. However, it seems that this does not affect the validity of our main conclusions concerning the dynamic properties of dust particles and they can be applied in our simulations. Thus we will assume that the temperature characterizing the kinetic energy of dust particles in our case is equal to the neutral gas temperature and use the expression for the friction coefficient appropriate for the kinetic region.

III. CHARGING OF DUST GRAINS

For simplicity in our simulations we will proceed with the assumption that dust particles immersed in a plasma already have equilibrium charge. To justify this assumption we show that the characteristic time of dust grain charging in our conditions is much less than the simulation time step. In our experiment the dust grain is charged by collecting electrons and ions from plasma and by emitting electrons due to thermal emission from the hot dust surface. For the ion and electron flows to the particle surface we can write (assuming the positive grain charge)

$$I_e^+ = e\,\frac{\pi a^2}{4}\,n_e\sqrt{\frac{8T_g}{\pi m_e}}\left[1 + \frac{2Q_d e^2}{aT_g}\right], \tag{9}$$

$$I_i^+ = e\,\frac{\pi a^2}{4}\,n_i\sqrt{\frac{8T_g}{\pi m_i}}\exp\left(-\frac{2Q_d e^2}{aT_g}\right), \tag{10}$$

where $n_{e(i)}$ and $m_{e(i)}$ are the electron (ion) density and mass, respectively. The electron flow from the particle surface can be given by [15]

$$I_e^- = e\,\frac{\pi a^2}{2}\left(\frac{mT_g}{2\pi\hbar^2}\right)^{3/2}\sqrt{\frac{8T_g}{\pi m}}\left[1 + \frac{2Q_d e^2}{aT_g}\right] \times \exp\left(-\frac{W_e}{T_g}\right)\exp\left(-\frac{2Q_d e^2}{aT_g}\right), \tag{11}$$

where W_e is the work function, and we assume that the particle surface temperature is equal to the gas temperature. Particle charging is then determined by the following differential equation:

$$\frac{dQ_d e}{dt} = I_e^- + I_i^+ - I_e^+ . \tag{12}$$

One can see from Eqs. (9) and (10) that $I_e^+/I_i^- \geqslant \sqrt{m_i/m_e} \gg 1$, so that ion collection may be neglected. The steady state charge is then determined by equating $I_e^- = I_e^+$, to give $Q_d \approx 550$, for the conditions obtained in the experiment ($T_g = 1700$ K, $a = 0.8$ μm, $n_e = 7 \times 10^{10}$ cm^{-3}, $W_e = 2.1$ eV [6]). This charge is very close to $Q_d \approx 500$ determined from the charge balance $n_e = n_i + Q_d n_p$. Equation (12) can be solved numerically and the characteristic time of charging can be evaluated. This time turns out to be very small. For example, under the same conditions we obtain that the time

needed to acquire 90% of equilibrium charge is about 10^{-10} s. The simulation time step is several orders greater so our assumption is justified.

IV. NUMERICAL SIMULATIONS

The numerical simulations have been carried out by means of code KARAT [16] using the molecular dynamics method in 2D geometry. It includes solution of the equation of motion for each dust grain taking into account the interaction between dust grains, friction force, and random force arising from asymmetric molecular bombardment (the Brownian force):

$$m_d \frac{d^2\vec{r}_k}{dt^2} = \sum_j \Phi(r)|_{r=|\vec{r}_k-\vec{r}_j|} \frac{\vec{r}_k-\vec{r}_j}{|\vec{r}_k-\vec{r}_j|} - m_d \nu_{\rm fr} \frac{d\vec{r}_k}{dt} + \vec{F}_{\rm Br} \tag{13}$$

where m_d is the grain mass, $\nu_{\rm fr}$ is the friction decrement, and $F_{\rm Br}$ is the random force providing the Brownian motion. $\Phi(r)$ is taken in the following form:

$$\Phi(r) = \Phi_D(r) = -Q_d e \frac{\partial \phi_D}{\partial r}, \tag{14}$$

where

$$\phi_D = \frac{Q_d e}{r} \exp\left(-\frac{r}{d}\right). \tag{15}$$

Here d is the Debye length and ϕ_D is the Debye potential. It should be noted that the system under consideration can be studied with MD without friction and Brownian forces (see, for example, [17]). However, theses forces represent a physical process and some results [18] indicate that they may have important effects on ordering structure formation.

The computation area is of square form with the side length L_0. In order to emulate an infinite system we use periodic boundary conditions, so that the basic simulation area is surrounded by neighboring copies of itself, and each particle in the basic computation area interacts not only with the particles in the basic area but also with the ''mirror'' particles. The emergence of the grains leaving the basic computation square on its opposite edge is also included. Such periodic boundary conditions give the possibility of avoiding boundary effects and fix the mean dust density. Initially charged dust grains are situated in random positions inside the computation area after which the process of self-organization starts. Such consideration corresponds to the real process in experiment where initially neutral and disordered dust grains come into the plasma region, acquire electric charge very quickly (Sec. III) and start interacting.

The 2D dust density is chosen for the mean intergrain distance l to be equal to the distance calculated from experimental 3D dust density $n_d : l = (4\pi n_d/3)^{-1/3}$. In this case one can expect the simulation of the processes in 2D geometry to be realistic. In practice one had to limit the real interaction, associated with the screened Coulomb potential (15) on too small distances. It is clear that initial positions of some grains may be extremely close together with very high initial interaction force, which would demand too small a time step. In order to avoid this problem the interaction force was limited on distances less than $l_0 = 0.3l$. Actually it does not affect the ordering process because computer simulation shows that after several first time steps there are no particles separated by distance less than l_0. Thus the following interaction law was used in the simulation instead of a realistic one:

$$\tilde{\Phi}(L) = \begin{cases} \Phi(l_0) & \text{if } L < l_0 \\ \Phi(L) & \text{if } l_0 < L. \end{cases} \tag{16}$$

TABLE I. Parameters used in numerical simulations corresponding to the conditions of the experiment.

$T_g = 1700$ K	$P = 1$ Bar	$Q_d = 500$
$n_e = 7\times10^{10}$ cm^{-3}	$n_i = 4\times10^{10}$ cm^{-3}	$n_d = 5\times10^{7}$ cm^{-3}
$l = 17$ μm	$d = 11$ μm	$a = 0.8$ μm
$m_d = 1.6\times10^{-12}$ g	$\nu_{\rm fr} = 9.6\times10^{4}$ s^{-1}	$\Gamma = 150$
$\Gamma_D = 30$	$N = 200$	$\tau_s = 0.3$ μs

Parameters for the simulation (listed in Table I) are chosen according to the conditions of the experiment in which the existence of dust ordered structure was observed. In Table I N is the number of particles in the simulation and τ_S is the simulation time step. The dust mass is $m_d = (\pi/6)\rho_d\ a^3$ with $\rho_d = 6$ g/cm^3 being the density of the dust matter CeO_2. According to results of Sec. II the temperature that characterizes dust grain kinetic energy was taken to be equal to that of the gas and the expression for $\nu_{\rm fr}$ appropriate for the kinetic region was used:

$$\nu_{\rm fr} = \frac{2}{3}\frac{Pa^2}{m_d}\sqrt{\frac{2\pi M}{T_g}}. \tag{17}$$

One can compare the deceleration time $1/\nu_{\rm fr} \approx 10$ μs with that of the structure formation t_f, which is tens of milliseconds, to find $t_f \nu_{\rm fr} \gg 1$. This means that the inertia is essentially negligible in the regular motion of the grains caused by interaction forces. Unfortunately it is impossible to exclude the inertial term from Eq. (13) because the simulation of the Brownian motion is impossible without it. The time step τ_s should be less than $1/\nu_{\rm fr}$ to simulate Brownian motion accurately; in particular, $\tau_s = 0.03/\nu_{\rm fr}$ was taken with 250 000 time steps being executed during the simulation. This is the reason why the 2D approach was utilized with a relatively small number of grains ($N = 200$). A larger number would require too much computing time. Nevertheless, this seems to be enough to take into account that the medium with a moderate value of Γ was investigated where the correlation radius does not exceed several l.

As can be seen from Table I the ion density is small compared with the electronic one. It should be noted that the definition of Debye length in plasma with such a large dust density is not clear. This problem requires special analysis, which is beyond the scope of this paper. In the work presented d was calculated in a simple way just neglecting ion shielding: $d = \sqrt{T_e/(4\pi e^2 n_e)}$. The coupling parameters Γ, Γ_D were calculated through the formulas

$$\Gamma = \frac{{Q_d}^2 e^2}{l T_d}, \quad \Gamma_D = \frac{{Q_d}^2 e^2 \exp(-l/d)}{l T_d}. \tag{18}$$

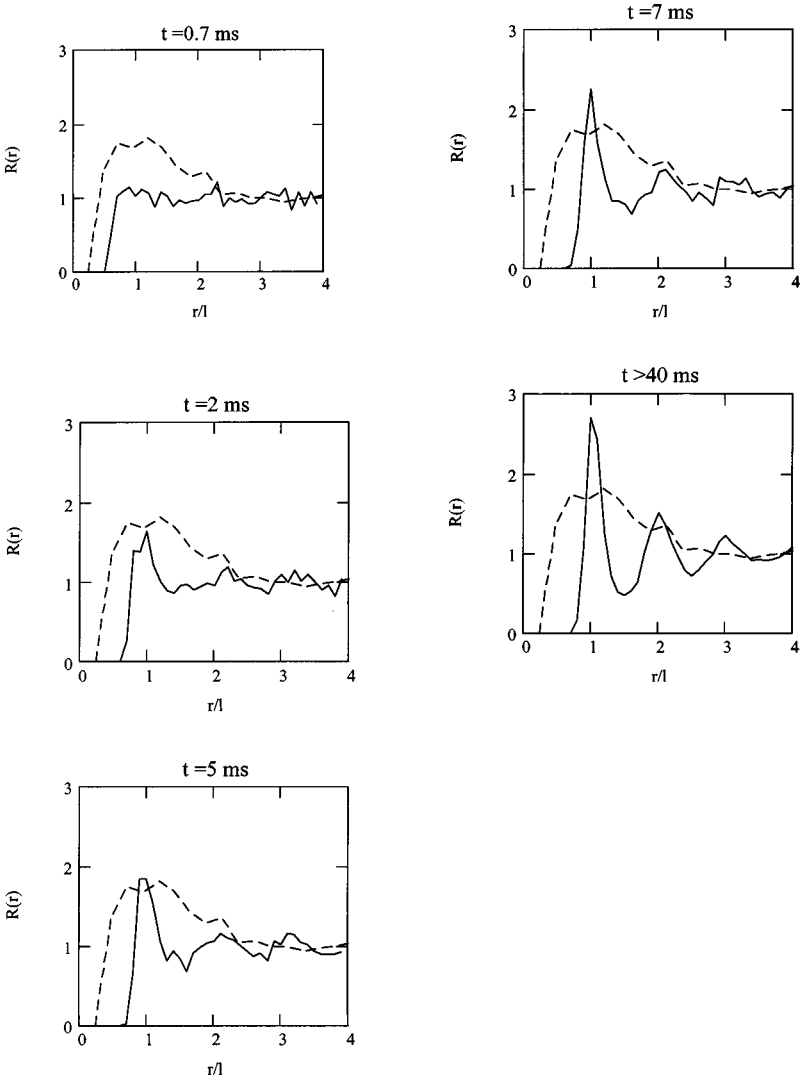

FIG. 3. The time evolution of the correlation function in the numerical simulation. The solid curve corresponds to the simulation, the dashed line to the correlation function obtained in the experiment.

Simulation has shown that after some relaxation process the system approaches the final stationary stage corresponding to the liquidlike state. This agrees with the values of the coupling parameters Γ,Γ_D. Figure 3 presents the time evolution of the pair correlation function $R(r)$ calculated from the grains positions at the moment taken. The last picture in Fig. 3 was obtained through time averaging of R, which is possible because on the final stage of the simulation ($40<t<70$ ms) the system approach to the equilibrium state and the pair correlation function does not evolve in time. In the calculation of the pair correlation function the step along r was taken to be $0.1l$, a smaller one would result in too large of a chance of calculation error. The grain distributions on the computation area obtained in the simulation are given in Fig. 4.

One can see from Fig. 3 that, first of all, the particles at small distances disappear with the area of zero correlation function at small r being formed. This process takes place very quickly because the electric repulsive force at small distance is very strong. Then the sharp nearest-neighbor peak develops ($t=5$ ms). Further, this peak grows and simultaneously the high-order peaks develop. The final correlation

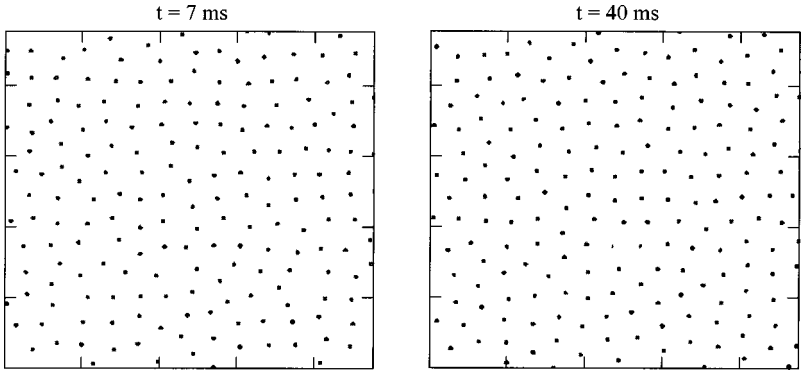

FIG. 4. Dust structures obtained in the numerical simulation. The image on the left represents the formation stage corresponding to the plasma flight time in the experiment; the image on the right represents the final state of the dust system under thermal equilibrium.

function is characterized by many sharp oscillations. The definition of the structure formation time t_f remains to some extent uncertain because it depends on the distance range where the evolution of the correlation function is of interest. The bigger the distance the longer the time required for the correlation function to approach the final form at this distance. In practice one may take into account only the distance range where the appreciable oscillations of the final correlation function take place. In the case at hand one may take only the first three peaks, then t_f can be estimated $t_f \approx 35$ ms. Also, it is convenient to introduce the time of the sharp nearest-neighbor peak emergence t_1. This is in fact the time required for any type of short order to appear in the system. One can estimate from the simulation that $t_1 \approx 5$ ms. This time can be also estimated analytically:

$$t_1 \approx \frac{l m_d \nu_{\rm fr}}{|\Phi(l)|}, \tag{19}$$

which gives $t_1 \approx 25$ ms. The inaccuracy of this estimation is related to strong dependence of the interaction force on distance because of Debye screening. The initial ordering stage is related to the grains diverging on small distance $r < l$. Substituting $0.7l$ instead of l in Eq. (19) one would obtain $t_1 = 6$ ms, in good agreement with the simulation.

As was stated in the Introduction the flight time of dust grains in the experiment is $t_{\rm ft} = 7$ ms $< t_f$. This means that the pair correlation function measured in the experiment corresponds to the forming structure. The flight time is large enough for the short order to appear but it is not enough for the correlation function to approach its final form with many oscillations. Let us compare the simulation correlation function with the experimental one (Fig. 3). Two obvious specific features of the experimental correlation function can be seen. First, it has only one peak. It agrees with the simulation results, one can see that at time $t = 7$ ms the magnitude of high-order peaks is approximately two times less than on final stage, while the main peak is already close to its final form. Thus the absence of high-order peaks of the experimental pair correlation function can be caused by the nonstationary character of the structure concerned.

The second specific peculiarity of the experimental correlation function is that the peak is extremely wide. Its width is almost five times larger than in the simulation. It should be stressed that such a wide peak is generally unusual for liquid systems. The most plausible reason for this broadening is the local inhomogeneity of the dust structure. It is clear that in the case when the dust density varies along the structure the peak of the correlation function should be broadened because of l variation in space. The mechanism of such inhomogeneity generation remains unclear now and requires special analysis that is beyond the scope of this paper. Anyway it is obvious that inhomogeneity concerns are not related to the process of structure ordering caused by electric intergrain interaction.

V. CONCLUSION

Thus the simulation results presented show that ordering of the dust structure manifested in the experiment [6] can be explained by the electric interaction of dust grains. It is found that the structure obtained in the experiment is far from equilibrium because the plasma flight time is less than the time of structure formation. It conforms to the emergence of the experimental correlation function characterized by a sharp main peak with no high-order ones.

At the same time the comparison of the simulation correlation function with the experimental one indicates some discrepancy, in particular, the peak of the experimental correlation function is extremely wide, which does not agree with the simulation results and in general seems to be unusual for known liquid structures. This peak broadening is likely to be related to the structure inhomogeneity, the generation mechanism of which requires special investigation.

The simulation of the ordering process presented has required the specification of some parameters involved. It is shown through the experimental measurements of the diffusion coefficient that the thermal energy of dust grains is close to the gas temperature and the friction force acting on grains is determined via the expression obtained in the kinetic limit. The analysis of dust charging shows very small charging time for experimental conditions. In practice one may consider that grains acquire charge instantly once they enter the flame region.

ACKNOWLEDGMENTS

We wish to thank Dr. A. A. Samarian and A. M. Lipaev for their assistance in taking some of the measurements. We are grateful to Dr. John Luthe for useful corrections to the manuscript. This work was supported in part by the Russian Foundation for Basic Research Grant No. 95-02-06456 and by INTAS-RFBR Grant No. 95-1335.

[1] J. H. Chu and Lin I, Phys. Rev. Lett. **72**, 4009 (1994).
[2] H. Thomas *et al.*, Phys. Rev. Lett. **73**, 652 (1994).
[3] Y. Hayashi and K. Tachibana, Jpn. J. Appl. Phys., Part 1 **33**, L804 (1994).
[4] A. Melzer, T. Trottenberg, and A. Piel, Phys. Lett. A **191**, 301 (1994).
[5] V. E. Fortov *et al.*, Phys. Lett. A **229**, 317 (1997).
[6] V. E. Fortov *et al.*, Phys. Lett. A **219**, 89 (1996).
[7] H. Thomas and G. E. Morfill, in *Proceedings of the Sixth Workshop on the Physics of Dusty Plasmas*, edited by P. K. Shukla, D. A. Mendis, and V. W. Chow (World Scientific, Singapore, 1996), p. 199.
[8] A. Melzer, A. Homann, and A. Piel, Phys. Rev. E **53**, 2757 (1996).
[9] H. Thomas and G. E. Morfill, Nature (London) **379**, 806 (1996).
[10] J. B. Pieper and J. Goree, Phys. Rev. Lett. **77**, 3137 (1996).
[11] P. N. Pusey and R. T. A. Tough, in *Dynamic Light Scattering: Application of Photon Correlation Spectroscopy*, edited by R. Pecora (Plenum, New York, 1985).

[12] K. Shatzel, Adv. Colloid Interface Sci. **46**, 309 (1993).
[13] G. B. King, C. M. Sorensen, T. W. Lester, and J. F. Merklin, Appl. Opt. **21**, 976 (1982).
[14] M. R. Zacharian, D. Chin, H. G. Semerjian, and J. L. Katz, Appl. Opt. **28**, 530 (1989).
[15] M. Sodha and S. Guha, Adv. Plasma Phys. **4**, 219 (1971).
[16] V. N. Tsytovich, R. Bingham, Ya. K. Khodataev, and V. P. Tarakanov, in *Advances in Dusty Plasmas*, edited by P. K. Shukla, D. A. Mendis, and T. Desai (World Scientific, Singapore, 1997), p. 212.
[17] M. J. Stevens and M. O. Robbins, J. Chem. Phys. **98**, 2319 (1993).
[18] X. H. Zheng and J. C. Earnshaw, Phys. Rev. Lett. **75**, 4214 (1995).